Published online 26 November 2014 *Nucleic Acids Research, 2014, Vol. 42, No. 22* ***13633–13645***
doi: 10.1093/nar/gku1190

Replication-guided nucleosome packing and nucleosome breathing expedite the formation of dense arrays

Brendan Osberg[1,†], Johannes Nuebler[1,†], Philipp Korber[2] and Ulrich Gerland[1,*]

[1]Theory of Complex Biosystems, Physik-Department, Technische Universität München, James-Franck-Strasse 1, D-85748 Garching, Germany and [2]Adolf-Butenandt-Institut, University of Munich, Schillerstrasse 44, 80336 Munich, Germany

Received August 19, 2014; Revised October 30, 2014; Accepted November 3, 2014

ABSTRACT

The first level of genome packaging in eukaryotic cells involves the formation of dense nucleosome arrays, with DNA coverage near 90% in yeasts. How cells achieve such high coverage within a short time, e.g. after DNA replication, remains poorly understood. It is known that random sequential adsorption of impenetrable particles on a line reaches high density extremely slowly, due to a jamming phenomenon. The nucleosome-shifting action of remodeling enzymes has been proposed as a mechanism to resolve such jams. Here, we suggest two biophysical mechanisms which assist rapid filling of DNA with nucleosomes, and we quantitatively characterize these mechanisms within mathematical models. First, we show that the 'softness' of nucleosomes, due to nucleosome breathing and stepwise nucleosome assembly, significantly alters the filling behavior, speeding up the process relative to 'hard' particles with fixed, mutually exclusive DNA footprints. Second, we explore model scenarios in which the progression of the replication fork could eliminate nucleosome jamming, either by rapid filling in its wake or via memory of the parental nucleosome positions. Taken together, our results suggest that biophysical effects promote rapid nucleosome filling, making the reassembly of densely packed nucleosomes after DNA replication a simpler task for cells than was previously thought.

INTRODUCTION

In eukaryotic cells, DNA is packaged into chromatin with nucleosomes as the basic building blocks. A high nucleosome coverage is essential for cells, for example to prevent cryptic transcription (1). In addition, the local positions of specific nucleosomes, especially in promoter regions, can affect transcription factor binding and thereby play an important role in gene regulation (2–5). Nucleosomes consist of about 147 bp of DNA wound around an octamer of histone proteins. While the length of linker DNA connecting neighboring nucleosomes varies locally, nucleosome mapping experiments (6–8) indicate an overall nucleosome coverage of around 90% in yeasts (i.e. the fraction of base pairs of the genomic DNA that are nucleosomal). This dense packing of nucleosomes has to be re-established whenever the DNA is (partially) cleared of nucleosomes, for instance during transcription, repair and replication. This is particularly challenging in the case of replication where the doubled amount of DNA needs to be assembled into chromatin. It is of interest how cells achieve this assembly within biologically reasonable timescales.

A related physical process, the sequential adsorption of mutually exclusive particles from a bulk solution onto a lower-dimensional substrate, has been intensely studied in non-equilibrium statistical physics (9). In a simple one-dimensional model, sometimes referred to as the 'car parking' model, particles can bind to an initially empty line at any position where they do not overlap with particles already in place (10,11). If the adsorption is irreversible, all gaps larger than the particle size are quickly occupied and the coverage then runs into a 'jamming' plateau where nearly 75% of the line is covered (12). If the process is reversible, that is, if desorption is allowed, the density can be increased beyond this limit. Density increases then happen via rare events where a 'bad parker', a particle whose neighboring voids taken together are larger than the particle size, detaches and is replaced by two particles. This process is kinetically limited by the desorption rate, since at least one desorption event must precede any density increase. While the frequency of particles arriving at the substrate and attempting to adsorb must be much larger than the desorption rate to obtain high coverage, increasing it even further,

*To whom correspondence should be addressed. Tel: +49 (89) 289 - 12394; Fax: +49 (89) 289 -14656; Email: gerland@tum.de
†The authors wish it to be known that, in their opinion, the first two authors should be regarded as Joint First Authors.

e.g. via increase of the particle concentration in bulk solution, will not speed up the filling process. Instead, the adsorption rate merely sets the final density that is eventually achieved.

It was shown by Padinhateeri and Marko (13) that the jamming plateau can pose a serious kinetic challenge to the formation of dense nucleosome arrays: based on an *in vitro* measurement of the nucleosome formation rate (14) and a discrete version of the above-mentioned one-dimensional adsorption-desorption model that describes the nucleosomes as impenetrable particles covering 147 bp of DNA, they concluded that the physiological coverage of 90% of the DNA cannot be reached on biologically reasonable timescales without additional mechanisms. They also showed that an additional remodeling mechanism, which moves a nucleosome along the DNA in a randomly selected direction until it collides with its neighbor, can eliminate the kinetic problem and yield high coverage beyond the jamming plateau on much shorter timescales.

Here we show that the jamming problem is alleviated by the 'softness' of nucleosomes and by replication-guided nucleosome packing. We consider nucleosomes soft when the full-size footprints of neighboring nucleosomes can overlap. Such overlaps can arise by two different means: first, nucleosomes are known to breathe, i.e. nucleosomal DNA partially unwraps from the histone core, leading to a dynamic footprint on the DNA. Thermal fluctuations are sufficient to mediate transient unwrapping *in vitro* (15–17), while adenosine triphosphate-dependent chromatin remodeling enzymes (18) also affect unwrapping *in vivo* (19–21). Second, nucleosome assembly occurs in a stepwise manner, with an H3/H4 tetramer deposited first, followed by the addition of two H2A/H2B dimers (22). Effectively, the assembly process therefore leads to a transiently reduced DNA footprint. Taken together, nucleosome breathing and stepwise assembly permit neighboring nucleosome dyads to be more closely spaced than the canonical 147 bp footprint length, albeit with a reduced probability. There is indeed considerable genomic evidence for this behavior, including a direct experimental confirmation of the mutual invasion of neighboring nucleosomal DNA territories (23), and statistical evidence from the analysis of nucleosome maps (24,25).

Nucleosome softness necessitates a theoretical description that goes beyond treating nucleosomes as impenetrable 'hard-core' particles. A 'Soft-core Nucleosome Gas' (SoNG) model was previously introduced as a generalization of the Kornberg–Stryer model (26) for the analysis of gene-averaged steady-state nucleosome positioning patterns (24). To study the effects of nucleosome softness on the above-mentioned jamming problem, we introduce here a kinetic model that reproduces the steady state pattern of the SoNG model, but also describes the 'nucleosome filling dynamics', i.e. the approach to the steady state. We contrast the dynamic behavior of our kinetic SoNG model with that of the corresponding hard-core model that was previously studied (13,27). The comparison is justified, in the relevant parameter regime, by the observation that the steady-state nucleosome patterns of the two models are essentially the same and are both compatible with yeast data (24). We find that dense nucleosome arrays form much faster within the SoNG model, which proceeds via a new 'cramming' regime, avoiding the jamming behavior of hard-core nucleosomes.

In the second part of this article, we then explicitly consider nucleosome filling in the context of DNA replication. In yeast, replication starts at many origins across the genome and proceeds at rates that are highly variable, with 50 bp/s marking a typical speed of the replication fork (28). Most of the existing parental nucleosomes are directly passed on to the daughter strands (29). The essential steps of this 'segregation' process are removal and partial disassembly ahead of the fork, allocation to one of the daughter strands, and reassembly onto the daughter strand (30–32). *De novo* assembly of the missing nucleosomes then re-establishes densely packed chromatin behind the fork. The parental nucleosomes are deposited closely behind the fork (33) and typically within a distance of <400 bp from their parental loci (34), mediated by spatial association of the involved chaperones with the replication fork (31). Nucleosome positioning patterns appear to be virtually identical ahead of and behind the fork (35). There is some evidence that nucleosomes are distributed between the daughter strands in a random fashion with roughly equal shares (33,36,37), but the details of this process are still unclear and appear to be context dependent (38). Also, the process may differ between the leading and the lagging strand (39).

Taken together, the experimental evidence suggests that the segregation of parental nucleosomes is an orchestrated process that happens in close proximity to the fork, while the *de novo* deposition is less coordinated and less spatially constrained. We explore the interplay between a processively moving replication fork, nucleosome segregation and *de novo* assembly of nucleosomes on the newly synthesized DNA. We devise two simplified model scenarios intended to expose generic consequences of this interplay. Our model illustrates that nucleosome filling is facilitated by replication guidance in two cases, (i) if nucleosome (re)assembly behind the replication fork is sufficiently rapid to suppress the transient occurrence of large gaps and (ii) if the segregation process is highly orchestrated, e.g. such that the placement of parental nucleosomes alternates between the daughter strands and their new positions are highly correlated with their parental positions. In the first case, jamming is avoided by sequential filling, while positional 'memory' circumvents jamming in the second case.

MATERIALS AND METHODS

We first introduce our model for the assembly of nucleosome arrays on a large segment of naked DNA, and then extend it to a minimal model of replication-guided nucleosome filling. The starting point for the construction of our model, and a point of reference for its analysis, is a previously studied assembly model for nucleosome arrays (13), which is a kinetic version of the Kornberg–Stryer model (26). The DNA is represented as a one-dimensional lattice, with each lattice site representing a single base pair. Nucleosomes are assembled and evicted at random locations with the only constraint that gaps <147 bp wide cannot be filled. The steady-state of these kinetics is the statistical nucleosome distribution of the Kornberg–Stryer model, with the steady-state nucleosome density $\overline{\rho}$ set by the rates for assem-

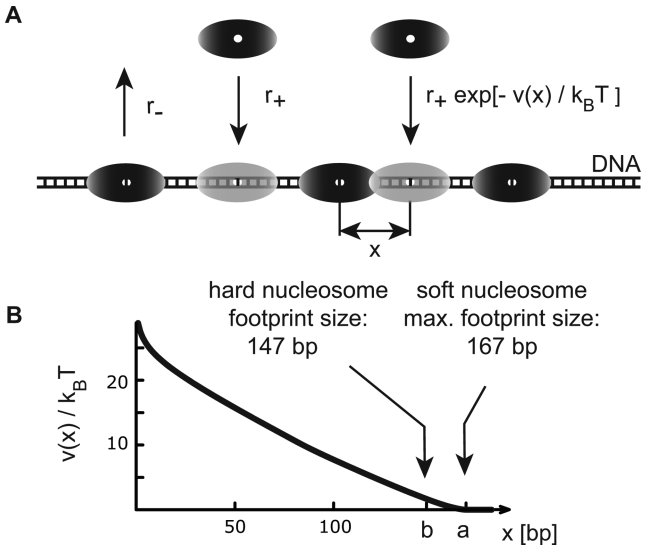

Figure 1. Kinetic model for the assembly of soft-core nucleosomes into dense arrays. (**A**) Nucleosomes (illustrated by shaded ellipses) are assembled onto free DNA at a rate r_+ and are evicted at a rate r_-. Nucleosomes can also form if this leads to an overlap of their DNA footprints, but the on-rate is then reduced by the Boltzmann factor of the interaction energy $v(x)$. Here, x denotes the distance between dyads, i.e. the center positions within nucleosome footprints (hollowed out in the nucleosome symbol). (**B**) The interaction potential $v(x)$ of soft-core nucleosomes has a range of $a = 167$ bp, as opposed to hard-core nucleosomes which obey strict exclusion over a range of $b = 147$ bp.

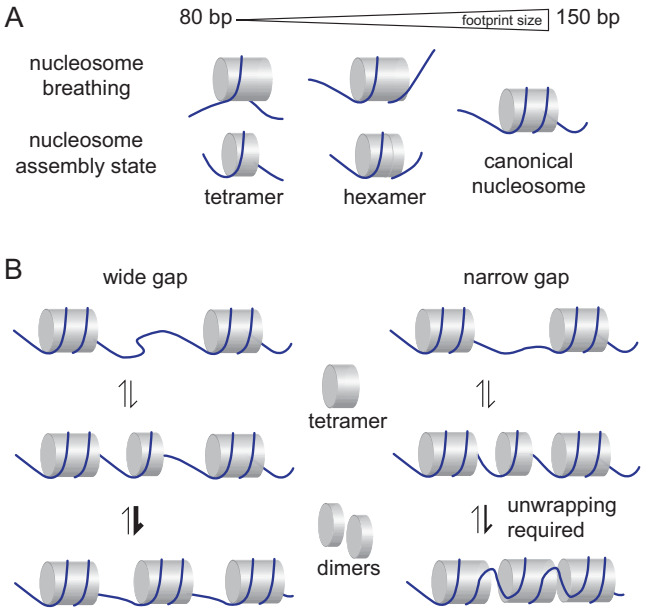

Figure 2. Nucleosome states with different DNA footprints and configuration-dependent nucleosome assembly. (**A**) Due to nucleosome breathing and multi-step assembly, nucleosomes have a multitude of internal states with a spectrum of DNA footprint sizes, i.e. they are 'soft'. In terms of DNA footprint size, the tetramer and hexamer states are equivalent to full nucleosomes with varying degree of DNA unwrapping. (**B**) The assembly rate of soft nucleosomes depends on the size of the gap between existing nucleosomes. Effectively, the stepwise assembly into a wide gap is faster than into a narrow gap, due to the required DNA unwrapping in the latter case.

bly and eviction, r_+ and r_-, via $\overline{\rho} = \eta/(1+\eta)$ with $\eta \exp(\eta) = r_+/r_-$, such that the steady-state density is a slowly increasing function of the rate ratio (11).

As illustrated in Figure 1A, we modify this model to take into account the softness of nucleosomes. The softness is manifested in a gradual repulsive potential between nucleosomes, shown in Figure 1B, which makes the assembly rate configuration-dependent, as opposed to the homogeneous assembly rate for hard-core repulsion. The rationale of our model is illustrated in Figure 2. Nucleosome softness stems from a multitude of structural states with different DNA footprint sizes, as depicted in Figure 2A. The statistical distribution of DNA footprint sizes is the essential determinant for the likelihood of assembling a nucleosome into a gap between existing nucleosomes. Within our model, the assembly into a narrow gap is less likely, but not excluded, as illustrated in Figure 2B.

The existence of nucleosome states with different DNA footprints is experimentally well established. Figure 2A depicts two classes of such states, those due to nucleosome breathing and those due to stepwise nucleosome assembly. Nucleosome breathing has long been suggested based on experiments showing that sites within the nucleosome footprint are accessible to binding proteins (15,40). Subsequently, the transient partial unwrapping of nucleosomal DNA from the histone core was directly demonstrated using single-molecule fluorescence techniques (16,17), and neighboring nucleosomes were shown to be capable of invading each others canonical 147 bp footprint (23). While these experiments were performed with reconstituted nucleosomes (via salt-gradient dialysis), indicating that thermal fluctuations are sufficient to produce transient unwrapping, ATP-dependent chromatin remodeling enzymes can also influence unwrapping *in vivo* (20,21). For our quantitative model, detailed below, it is important to note that nucleosome breathing leads to a rapid sampling of nucleosome states with different DNA footprints, with timescales in the millisecond to second regime (17).

According to the standard model for *in vivo* nucleosome assembly, an H3/H4 tetramer is first deposited onto the DNA and then completed to a full nucleosome by the addition of two H2A/H2B dimers (22,41). While there are different assembly pathways, both replication-coupled and replication-independent, involving different chaperones, remodelers and histone variants (22,30,31,42–44), the existence of assembly intermediates with reduced DNA footprint appears to be universal. Figure 2B (left panel) shows a simplified illustration of nucleosome assembly into a wide gap, where the neighboring nucleosomes do not impose any constraints on the assembly. The involved chaperones and remodelers are not shown in the illustration. In our quantitative model, we will use effective rates, which subsume all factors that affect these rates. Both assembly steps, formation of a tetrasome and integration of the heterodimers, are depicted as reversible processes; the backward reactions correspond to nucleosome eviction (18,45,46). Given that fully assembled nucleosomes are much more stable than assembly intermediates, the second step must be biased in the forward direction.

The right hand panel of Figure 2B illustrates the assembly into a narrow gap, where the neighboring nucleosomes affect the assembly process. This should primarily affect the rate of heterodimer integration in the second step, which requires DNA unwrapping in at least one of the shown nucleosomes (it does not matter how the required amount of unwrapping is distributed between the nucleosomes). The general implication for the construction of our quantitative model below is that soft nucleosomes, which feature an intrinsically variable DNA footprint size, will assemble at a rate that depends on the size of the gap between the existing neighboring nucleosomes, no matter if the newly deposited nucleosome enters as a breathing nucleosome or as some intermediate of stepwise assembly. For our purpose of modeling the process of nucleosome array formation, it is then adequate to coarse-grain the assembly of a single nucleosome into a one-step process with a configuration-dependent rate. This leads us to the kinetic model illustrated in Figure 1A, with a constant nucleosome eviction rate r_- and a basal assembly rate r_+ that is modulated depending on the distances to the neighboring nucleosomes (we also consider the effect of a variable eviction rate, see below). Starting from an initial configuration, we are then interested in the approach to 'equilibrium' of this model, which corresponds to an ATP-dependent non-equilibrium steady-state of the real system (47).

We incorporate the effect of the neighboring nucleosomes onto the nucleosome assembly rate via a repulsive 'soft-core' interaction potential $v(x)$, which gradually reduces the rate with decreasing distance x. This constitutes an adiabatic approximation, justified by the observation that nucleosome breathing samples nucleosome states with different DNA footprint sizes on a rapid timescale (17). The form of $v(x)$ should be chosen such that it (i) relaxes the widespread assumption of hard-core nucleosomes, (ii) leads to steady-state nucleosome distribution compatible with *in vivo* nucleosome patterns and (iii) produces a spectrum of DNA footprints compatible with experiments probing the accessibility of nucleosomal DNA. The task of finding such a potential was already carried out in (24). There, a soft-core potential with two free parameters, representing the maximal nucleosome footprint size and the effective stiffness of nucleosomes, was used to construct a statistical model, the 'SoNG', to describe *in vivo* nucleosome patterns. It was found that this model provides a more consistent description of the nucleosome patterns across multiple yeast species than the corresponding hard-core nucleosome gas. The fit to twelve different yeast species led to an effective interaction footprint of $a = 167$ bp and a nucleosome stiffness of $\varepsilon = 0.15 k_B T$ per base pair. The latter is consistent with estimates obtained from *in vitro* nucleosomal DNA accessibility data (48). The former is 20 bp longer than the DNA within a nucleosome core particle, which is not surprising, since steric constraints should disfavor neighboring nucleosomes with no linker DNA in between. Figure 1B shows the best-fit potential $v(x)$, with x measuring the dyad-to-dyad distance between neighboring nucleosomes.

The explicit shape of the potential is derived from the assumption of a constant energetic cost ε per bp to reduce the maximal DNA footprint a of a nucleosome at each end. For two neighboring nucleosomes placed with a dyad-to-dyad distance $x < a$, the required total footprint reduction can be distributed between the two nucleosomes and all possibilities are statistically weighted with the Boltzmann factor. Reference (24) finds that the simple expression

$$v(x) \approx (a - x)\epsilon - k_B T \ln\left[1 + (a - x)\left(1 - \mathrm{e}^{-\epsilon/k_B T}\right)\right] \quad (1)$$

for $x \leq a$ and $v(x) = 0$ for $x > a$ is an excellent approximation to this statistical average. Given that the values of its parameters a and ε were determined from *in vivo* data and yield a consistent description of gene-averaged nucleosome patterns over a range of yeast species, this potential essentially captures all effects that contribute to these steady-state patterns, including the action of remodelers. However, the fact that it is also consistent with the *in vitro* site-accessibility data suggests that thermal nucleosome breathing already leads to a similar sampling of footprint sizes as all *in vivo* processes combined. Therefore, equilibrium statistical models can be an adequate coarse-grained description of the 10-nm chromatin fiber even under *in vivo* conditions where it is an active system, contrary to what has been claimed elsewhere (27). We also note that our parameters for the maximal footprint and the unwrapping energy per base pair are compatible with those independently estimated from a different dataset (25). This analysis also considered an additional oscillatory component in the unwrapping energy to reflect the known 10–11 bp periodic preference of nucleosome positions. However, the additional oscillatory component has a minor effect on the statistics of nucleosome positions, visible only in the statistics of the relative rotational positions of neighboring nucleosomes (25), but not in the average nucleosome patterns considered here.

The nucleosome assembly model introduced here defines the kinetics for the SoNG model of (24). The soft-core potential modulates the local nucleosome assembly rate into the effective rate

$$\tilde{r}_+ = r_+ \, e^{-[v(x_\mathrm{L}) + v(x_\mathrm{R})]/k_B T} , \quad (2)$$

where x_L and x_R are the dyad-to-dyad distances to the next nucleosome on the left and right, respectively. As above, r_+ denotes the rate of nucleosome assembly at a given position sufficiently far away from existing nucleosomes. While we also simply refer to it as the 'on-rate', it should be noted that r_+ is not an association rate in the usual sense, since it does not measure the frequency of binding events per concentration of binding molecules but already includes this concentration. In fact, it is currently unclear (to the best of our knowledge) whether r_+ is limited by the number of free histones or by the number of chaperones that assist the formation of nucleosomes. Our expression for the effective rate $\tilde{r}_+$ assumes that the interactions with the left and right neighbor are additive, which requires the unwrapping of the two DNA ends of a nucleosome to be independent. Although correlations (or anti-correlations) are certainly possible, e.g. due to cooperative effects or electrostatic interactions, we currently do not know of any clear experimental evidence indicating any significant correlation of this kind.

To reproduce the steady-state of the SoNG model, the nucleosome eviction rate (or 'off-rate') must be constant, such that $\tilde{r}_+/r_-$ is proportional to the Boltzmann factor of the interaction potential. We have chosen to assign the entire Boltzmann factor to the on-rate in Equation 2, but we will

also consider other choices in the 'Results' section. There, we show that assigning the entire Boltzmann factor to the on-rate is the most conservative choice, in the sense that another choice would support our claim of substantially faster nucleosome filling of soft nucleosomes even more. Finally, given that we do not study sequence-guided nucleosome positioning at specific genes here, Equation 2 neglects any dependence of the on-rate on the DNA sequence. For hard-core nucleosomes, such effects have been considered in (13).

Model extension for replication-guided nucleosome filling

To model nucleosome filling in the wake of a moving replication fork, we consider the same kinetics as described above, but with a system size L (length of the DNA in bp) that increases with time. Specifically, we add lattice sites at the right hand boundary with a constant rate v_{repl}. This moving boundary represents the replication fork, and nucleosomes can only form behind the fork. The interaction between nucleosomes and the replication fork is described in the same way as the interaction between nucleosomes, i.e. the boundary condition is as if an imaginary nucleosome would always sit with its dyad at position $L + 1$ (with L increasing in time). The same boundary condition is applied at the fixed left boundary, i.e. there is an imaginary nucleosome with dyad at lattice site 0.

We first assume that parental and newly synthesized nucleosomes are mixed in a common pool, but later separate them in order to study how memory of parental nucleosome positions can affect the filling kinetics. To that end, we initialize our model in a partially filled state, which is constructed using a minimal model for the inheritance of nucleosome positions: we assume that during replication each daughter strand obtains half of the parental histones, on average. Starting from a parental nucleosome configuration according to the steady-state, each nucleosome is placed in its exact parental position on one of the daughter strands, proceeding along the parental DNA. If the previous nucleosome was placed on strand 1, the next one is place on strand 2 with the 'alternation probability' α, and *vice versa*, such that $\alpha = 0.5$ corresponds to a completely random placement, while $\alpha = 1$ corresponds to perfect alternation. We then use one of these daughter strands as the initial state for nucleosome filling.

Model implementation and parameter choice

To determine the nucleosome filling kinetics, we perform kinetic Monte Carlo simulations using the Gillespie algorithm (49). In these simulations, the state of the system is specified by the list of bound nucleosome dyad positions. The transition rates between states depend on the configuration as described above. For the DNA lattice, we either use a linear geometry with hypothetical fixed particles at the two ends (for replication-guided nucleosome filling, see above) or periodic boundary conditions corresponding to circular DNA (in all other cases). In each case, the total DNA length L is chosen large enough to ensure that none of our observables display a significant finite size effect. Except for the case of inherited parental nucleosomes (see above), we use an empty lattice as the initial condition. All observables are averaged over a sufficient number of simulation runs to extract the mean kinetics (see Supplementary Table S2 for details). As our main observable, we calculate the average nucleosome density $\rho(t)$ as the number of nucleosomes divided by the total DNA length, i.e. it can be interpreted as the inverse of the average spacing between nucleosomes (in bp). The quantity $\rho(t)$ also corresponds to the average probability for a base pair to be occupied by a nucleosome dyad. As a second observable, we calculate the time-dependent nucleosome pattern close to a boundary or a reference nucleosome.

Table 1. Soft-core nucleosomes require a different ratio of on- to off-rate than hard-core nucleosomes to obtain the same steady-state nucleosome density. At high densities, the required ratio is dramatically larger for hard-core nucleosomes.

Model	$1/\bar{\rho}$ [bp]	r_+/r_-
Hard-core nucleosomes	155	3.69×10^6
	165	149
	180	2.37
Soft-core nucleosomes	155	4.57×10^3
	165	200
	180	5.70

While the steady-state nucleosome density depends only on the rate ratio r_+/r_-, we also need one of these rates in absolute terms in order to estimate the timescale of the filling kinetics. From constant-force measurements of the shrinking rate of DNA during nucleosome assembly in *Xenopus* egg extract (without ATP), the on-rate r_+ was estimated at $\sim 12\,s^{-1}$ for a DNA segment with length of one nucleosome footprint (14). However, this can at most be an order of magnitude estimate for our purposes, since the rate may be significantly different *in vivo* and in the presence of ATP (50). In all figures of this manuscript, time is therefore measured in units such that $r_- = 1$, and only a rough correspondence to real time is indicated. To obtain different asymptotic nucleosome densities, we adjust the rate ratio r_+/r_- as listed in Table 1. Note that the hard-core model requires a dramatically higher r_+/r_- ratio at high densities than the soft-core model. This observation is consistent with the previous finding that the hard-core model does not provide a unified physical description of the 10-nm chromatin fiber in different yeast species (24).

RESULTS

We now use the quantitative model described above to address our two main questions: how does the softness of nucleosomes affect the kinetics of nucleosome assembly into dense arrays? And under which conditions can the replication process assist in the rapid reassembly of dense nucleosome arrays?

Kinetics of assembling soft nucleosomes into dense arrays

Figure 3 shows a characterization of the nucleosome filling kinetics for both the hard-core and the SoNG model (labeled by HaNG and SoNG, respectively). Panels A and B plot the average nucleosome density, $\rho(t)$, as a function of time (with a logarithmic time axis). For the time axis, we

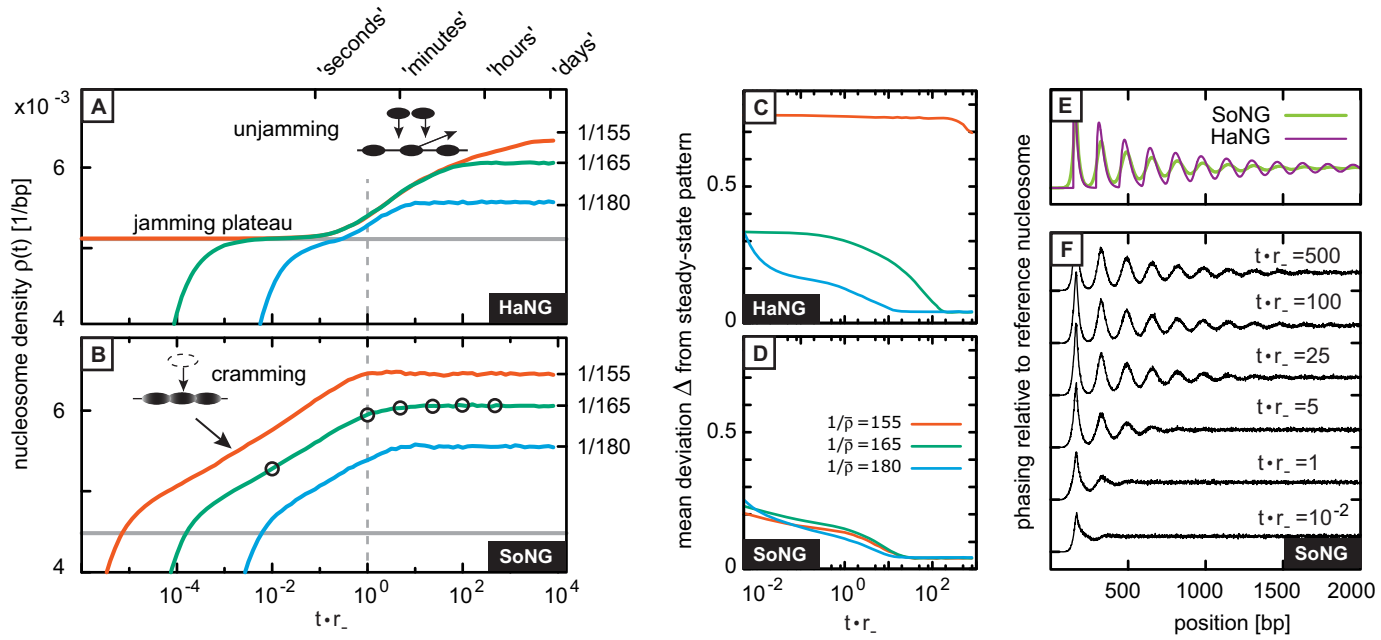

Figure 3. Characterization of nucleosome array assembly within the soft-core model and comparison to hard-core nucleosomes. (**A**) Time-dependent nucleosome density $\rho(t)$ for the HaNG model (with a logarithmic timescale). Three curves are shown for different final densities, as labeled on the right vertical axis. The gray horizontal line indicates the jamming density at which, statistically, non-overlapping adsorption opportunities have been exhausted. From this point, the hard-core nucleosomes must wait for desorption events to further increase the density (see sketch). The time labels above the figure mark approximate timescales based on the *in vitro* estimate of (13) (see main text). (**B**) Same plot for the SoNG model. Soft-core nucleosomes (represented by shaded ellipses in the sketch) have a larger maximal DNA footprint and accordingly have a smaller nominal jamming density (again indicated by a gray line). However, after reaching this density, $\rho(t)$ does not plateau, but instead enters a 'cramming' stage. (**C**) Mean deviation $\Delta(t)$ between the time-dependent nucleosome pattern $p(x, t)$ and its steady-state $\overline{p}(x)$ for the HaNG model (see text for details). The three curves correspond to the same cases as shown in panel (A). (**D**) Same plot for the SoNG model. (**E**) Comparison of the equilibrium patterns of the two models at a nucleosome density of 1/(165 bp). (**F**) Snapshots of the average nucleosome pattern during the filling process of the SoNG model for 1/(165 bp) final nucleosome density. The circles on the green line in panel B mark the points in time for which the snapshots are displayed.

use the average dwell time of a nucleosome on the DNA, $1/r_-$, as our time unit. The shape of the filling curves of the SoNG model in Figure 3B is strikingly different from that of the HaNG model in Figure 3A: initially, when the DNA coverage is still low, the density increases rapidly (linear in time) in both cases, since nucleosome–nucleosome interactions play a negligible role. Then, however, the filling of the hard-core model stalls, while the density steadily increases for the soft-core model. The stalling of the HaNG model occurs at a density of 1/197 bp, the 'jamming plateau' marked by the gray line. This plateau corresponds to a DNA coverage equal to the nontrivial theoretical limit of 74.8… % calculated by Rényi (12) for the irreversible random binding of equally sized objects to a continuous one-dimensional substrate. The continuum limit provides an accurate description also for our discrete DNA substrate, since nucleosomes are large compared to the discrete length unit of a single base. Importantly, the jamming plateau is independent of the on-rate: the three different curves in Figure 3A correspond to different r_+ values, but stall at the same coverage level, albeit at different times.

For the green traces in both Figure 3A and B, the on-rate is adjusted such that a steady-state nucleosome spacing of 165 bp is ultimately reached, corresponding approximately to the average spacing in *Saccharomyces cerevisiae* under physiological conditions (6). The blue traces illustrate the behavior for a reduced density with a 180 bp spacing, while the red traces illustrate the case of close to maximal packing with a 155 bp spacing. In the case of the HaNG model, nucleosome filling beyond the level of the jamming plateau starts at a timescale of $\sim 1/r_-$ for all three traces. This reflects the fact that 'unjamming' requires the removal of 'bad parkers', as illustrated in the sketch inside panel A. Note that for the green and red traces, the filling process is stalled for several orders of magnitude in time, and that unjamming is logarithmically slow (10).

Nucleosome filling within the SoNG model never stalls, but instead displays a 'cramming' stage. The crossover between the initial filling and the onset of cramming happens when most gaps are too small for further nucleosomes to attach at non-overlapping positions. This density is marked by the gray line in Figure 3B. The biophysics of the cramming process is analyzed in detail further below. On the phenomenological level, the cramming stage ends when the final steady-state density is reached, which happens on about the same timescale for all three traces. Remarkably, this timescale is not much longer than the unbinding timescale $1/r_-$, suggesting that breathing nucleosomes will reach dense packing already when hard-core nucleosomes are only starting the unjamming process. This conclusion is not dependent on the assumption, made in Equation 2, that the nucleosome–nucleosome interaction only affects the on-rate: as shown in Supplementary Figure S1, this assumption is conservative, since all other choices

for the dependence of the kinetics on the interaction (see Supplementary Text, Section I) only lead to even faster filling with soft-core nucleosomes.

Dynamics of nucleosome phasing

While the above analysis showed that a high density is reached very rapidly with soft-core nucleosomes, it did not address the question of whether the characteristic phasing of nucleosome arrays (7) forms on the same rapid timescale. We calculate the dynamics of nucleosome phasing via the time-dependent probability $p(x, t)$ of finding a nucleosome dyad at position x at time t, given that one reference nucleosome is fixed at position 0. To quantify the timescale of the approach to steady-state, we compute the normalized mean deviation Δ between the time-dependent pattern $p(x, t)$ and its steady-state limit $\overline{p}(x)$,

$$\Delta(t) = \frac{1}{L\overline{\rho}} \sum_{x=1}^{L} |p(x, t) - \overline{p}(x)| \, . \qquad (3)$$

Here, the steady-state limit $\overline{p}(x)$ is calculated exactly by the transfer matrix method as previously described (24), while $p(x, t)$ is obtained as an average over many kinetic simulations, see 'Materials and Methods' section and Supplementary Table S2.

Figure 3C and D show how the mean deviation Δ decreases as a function of time, for the HaNG and the SoNG model, respectively. The three different curves in each panel correspond to the same $\overline{\rho}$ values considered already in panels A and B. These curves demonstrate that the dynamics of the phasing pattern largely follow the behavior of the nucleosome density $\rho(t)$. For the HaNG model, the timescale of the approach to steady state increases dramatically with the steady-state density $\overline{\rho}$, whereas it displays no significant dependence on $\overline{\rho}$ for the SoNG model. Figure 3E superimposes the final pattern $\overline{p}(x)$ for the HaNG and SoNG model to show that the steady states of the two models are compatible with each other. Note that the sharp peaks in the pattern of the HaNG model are due to the exact positioning of the reference nucleosome; after taking into account the fuzziness in the positioning of e.g. the +1 nucleosome, the two patterns become almost identical and are both compatible with the genome-averaged experimental pattern of *S. cerevisiae* (24).

Figure 3F shows several snapshots of the dynamics of nucleosome phasing within the SoNG model, corresponding to the points marked by circles on the green curve in panel B. These snapshots illustrate how the phasing pattern emerges on the unbinding timescale $1/r_-$, by gradual propagation of the pattern from the reference nucleosome. Supplementary Figure S2 shows similar plots for other densities, and also for the HaNG model, which displays much slower dynamics consistent with Figure 3C. The slow dynamics of nucleosome pattern formation within the HaNG model were also observed in a recent study and motivated the extension of the model by an additional remodeling mechanism (27).

Physical analysis of the cramming stage

During the cramming stage in the nucleosome filling dynamics of Figure 3B, nucleosomes are 'squeezed' into progressively shorter gaps. The cramming stage begins when the average density $\rho(t)$ reaches the jamming density marked by the gray line in Figure 3B, i.e. the jamming density $\rho_c = 0.748/a$ for the maximal footprint a of the soft-core nucleosomes. At this point, the density $G_c(x)$ of internucleosome gaps of size x has the shape shown in Figure 4A. Here, x is measured as the distance between the dyads of neighboring nucleosomes and the gap density is plotted on a logarithmic axis. Note that despite the overall dependence of the filling dynamics on r_+, the distribution $G_c(x)$ at the onset of cramming is invariant, as shown in Supplementary Figure S3. To a good approximation, the shape of $G_c(x)$ is piecewise exponential with three regimes (see also Supple-

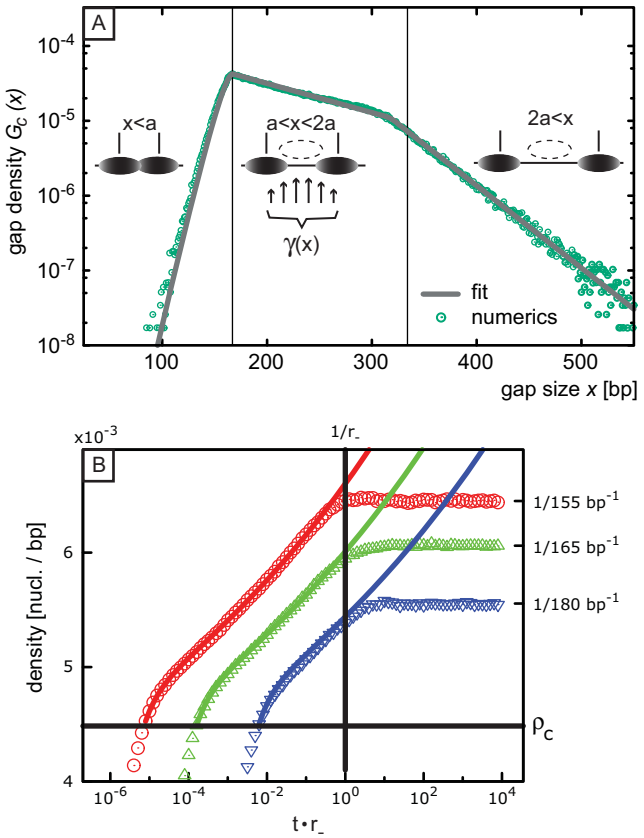

Figure 4. Analysis of nucleosome filling during the cramming stage of the SoNG model. (**A**) Length-dependent gap density, $G_c(x)$, at the onset of cramming on a logarithmic axis (the gap length x is measured as the distance between the dyads of neighboring nucleosomes). The green symbols show simulation data whereas the gray line shows the fit described in the main text. Vertical lines separate three regimes (see sketches for illustration): for $x < a$, neighboring particles already overlap, such that intervening adsorption will be strongly suppressed, due to an enormous energy penalty. The second regime, $a < x \lesssim 2a$, largely determines the cramming dynamics, with gaps that provide less than a nucleosome footprint of free DNA space. In the third region, $x \gtrsim 2a$, gaps are large enough to permit the assembly of an intervening nucleosome without interaction; these gaps will fill very quickly. All gaps fill with rate $\gamma(x)$ defined in Equation 5; the middle sketch illustrates how the different attachment possibilities within a gap sum up to the gap's total filling rate $\gamma(x)$. (**B**) Nucleosome filling during the cramming stage. Equation 4 (lines) describes the Monte Carlo simulations (symbols) throughout the cramming stage. See Table 1 for parameters. The horizontal gray line indicates the cramming density ρ_c, while the vertical gray line indicates the desorption timescale $1/r_-$, which marks the end of the cramming stage.

mentary Text, Section II): (i) for $x < a$, where the neighboring nucleosomes already overlap, the gap density increases roughly exponentially with gap size. The slope (gray line in Figure 4A) follows directly from the Boltzmann factor for the interaction potential. The addition of nucleosomes into gaps in this regime is exceedingly unlikely. (ii) For $x \geq a$, but less than an upper threshold $x^* \approx 2a$, the neighboring nucleosomes do not overlap, but the gap does not allow a new nucleosome to bind without significant interaction with at the least one of the existing nucleosomes. In this regime, $G_c(x)$ decays slowly with increasing gap size. (iii) For $x > x^*$, the gaps are wide enough to fit a new nucleosome without significant hindrance, such that only very few of these gaps remain at the onset of the cramming stage. Accordingly, the distribution $G_c(x)$ decays rapidly with x in this regime.

If the dominant kinetic process during the cramming stage is the filling of initially created gaps, we should be able to predict the dynamics of $\rho(t)$ from $G_c(x)$. Specifically, the time-dependent nucleosome density should follow

$$\rho(t) = \rho_c + \sum_x G_c(x) \left(1 - e^{-\gamma(x)(t-t_c)}\right) , \qquad (4)$$

where t_c is the time at which the nucleosome density reaches the cramming threshold ρ_c (defined above). As the total number of gaps in the system equals the number of nucleosomes, we also have the relation $\sum_x G_c(x) = \rho_c$. The factor in brackets corresponds to the probability that a gap of size x has been filled at time t, given a gap filling rate $\gamma(x)$. This rate can be obtained as the sum over the attachment rates at all positions between the dyads, with each position-specific rate according to Equation 2, such that

$$\gamma(x) = r_+ \sum_{x'=1}^{x-1} e^{[-v(x')-v(x-x')]/k_BT} \qquad (5)$$

(see also the sketch inside regime (ii) of Figure 4A). The cramming dynamics predicted by Equation 4 are shown in Figure 4B alongside the three simulated filling curves, displaying excellent agreement until the characteristic timescale $1/r_-$ for unbinding when the cramming stage ends. For the numerical evaluation of Equation 4, we used the entire distribution $G_c(x)$ (described as the piecewise exponential shown as the gray line in Figure 4A; see Supplementary Text, Section II for more details), however regime (ii) of the gap size distribution governs the cramming behavior (see Supplementary Figure S4 for an analysis of the relative contributions of the three regimes).

The above quantitative analysis confirms our biophysical interpretation of the cramming stage as a progressive filling of the gap distribution that is established prior to the onset of cramming. In other words, higher-order processes involving the recursive filling of newly created gaps are negligible. At the end of the cramming stage, when unbinding becomes relevant, the subsequent final equilibration occurs very fast in the SoNG model. This is due to the fact that after unbinding, the rebinding position of a nucleosome is not uniformly distributed within gaps, as is the case in the HaNG model. Rather, the energetic gradient of their interactions with neighboring nucleosomes provides a 'guiding funnel' toward proper spacing.

Nucleosome filling behind a moving replication fork

We now consider effects on the kinetics of nucleosome filling that can result from the process of DNA replication, using the model extension described in 'Materials and Methods' section. We first investigate a scenario where the DNA is cleared from nucleosomes by the replication fork and nucleosome filling of the daughter strands occurs behind the moving fork. The replication fork moves along the DNA with a certain speed v_{repl} and thereby exposes newly synthesized DNA continuously. Once the synthesized DNA has reached a sufficient length, a new nucleosome can assemble. If the progression speed is slow and the adsorption rate large, this will occur almost immediately when the new strand is long enough. Replication then continues and soon the next nucleosome can attach adjacent to the previous one. This leads to closely packed nucleosomes in the wake of the moving fork, as depicted in the upper part of Figure 5A. We refer to this as 'replication-guided' assembly. If, on the other hand, the replication fork progresses rapidly compared to the assembly rate, then large stretches of newly synthesized DNA will be exposed to nucleosome assembly at random positions, leading to jamming, as sketched in the lower part of Figure 5A. Note that in the limit of very fast replication, we would recover the replication-independent nucleosome filling studied above.

A typical replication speed is $v_{\mathrm{repl}} = 50$ bp/s or one-third of a nucleosome footprint per second, however a variation of at least a factor 10 in the replication speed has been observed (28). For the rate of nucleosome assembly, the extrapolated *in vitro* rate from (14) suggests 12 assembly attempts per second within a nucleosome footprint. Clearly, the *in vivo* rate could be substantially different and additionally modified by histone level and chaperone activity regulation. Given this spread in the relevant quantities, both of the above scenarios could be realistic. We therefore show a quantitative analysis of both regimes within the SoNG model in Figure 5.

Figure 5B shows the nucleosome density in the wake of the moving fork, while Figure 5C shows the time evolution of the density at a fixed position. In each case, a simulation result for a slow and fast replication fork is shown (see Supplementary Materials for more details). For slow replication (red traces), nucleosomes are packed tightly behind the fork. The density rises quickly after the fork has passed by and initially exceeds its ultimate equilibrium value. Later, the density decreases through events in which two nucleosomes leave and the gap is filled by only one nucleosome. In contrast, for fast replication (blue traces), the moving fork guides nucleosomes only weakly and the density follows the cramming behavior of naked DNA (black traces) in its last stage.

From the quantitative analysis in Figure 5 it becomes clear that the functionally ideal regime corresponds to an intermediate case where the replication-guided assembly directly leads to the steady-state density: if the assembly rate is tuned with respect to the replication speed, the nucleosomes behind the fork will already display the proper spacing, and the filling curve in Figure 5C will rapidly rise to the steady-state nucleosome density, without any overshoot or relaxation behavior. Such a fine-tuned optimal behavior

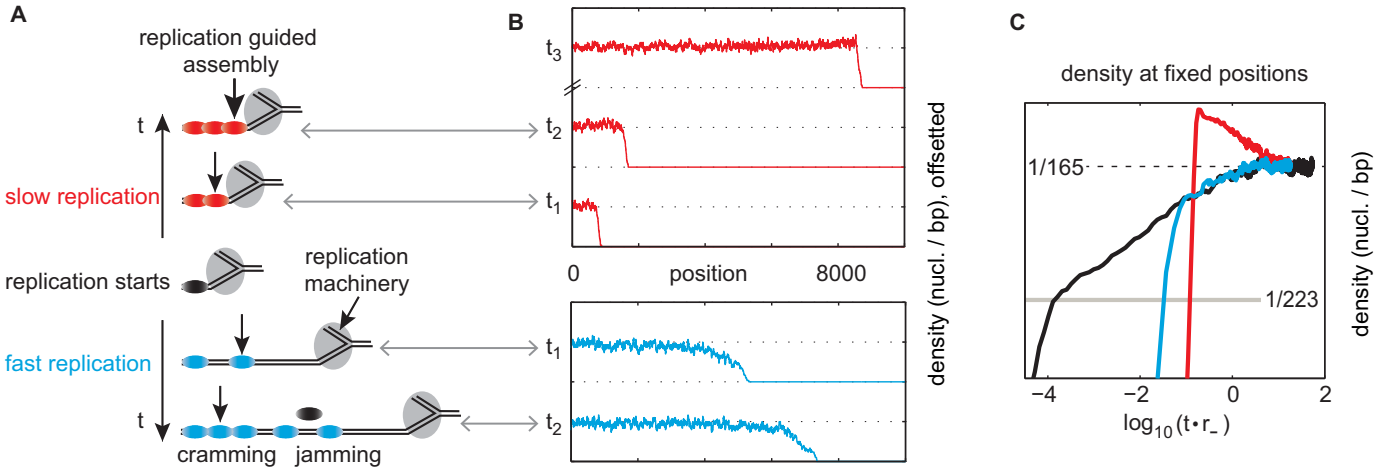

Figure 5. Illustration of the wake filling mechanism. (**A**) Schematic of different filling regimes in the wake of the moving replication fork (only one daughter strand shown). If the fork progresses slowly, or if replication machinery tightly replaces nucleosomes in its wake, nucleosomes attach to synthesized DNA very quickly once a sufficiently wide segment becomes available, leading to tight packing in the wake. If the fork progresses quickly, however, the newly synthesized DNA is left essentially empty. Jamming can then occur, which, for soft nucleosomes, is resolved by cramming. (**B**) Snapshots of the nucleosome density along the DNA at different times $t_1 < t_2 \ll t_3$. (**C**) Time-evolution of the nucleosome density at fixed positions. Time is set to zero when the fork passes by and filling can start. Red: for slow replication, the density initially exceeds and then approaches its equilibrium value. Blue: for fast replication the density in its final phase follows the replication-independent cramming behavior (shown in black for comparison). The cramming density ρ_c is indicated by the gray line. See Supplementary Figure S5 for detailed simulation parameters.

could be obtained, for instance, by coupling the replication speed to the concentration of free histones (see discussion for possible evidence).

Nucleosome filling guided by parental nucleosome positions

In the above analysis, parental and new nucleosomes were lumped together in one pool, from which nucleosomes were randomly placed on the newly synthesized DNA. To explore possible effects of nucleosome segregation on the filling kinetics, we now consider a variant of our model which takes the deposition of parental nucleosomes on the daughter strands into account. We assume that all parental nucleosomes are distributed between the daughter strands by the replication machinery, thus generating an initial state for the subsequent filling with new nucleosomes that is significantly different from the empty DNA assumed above. Given that important aspects of the nucleosome segregation process are not yet experimentally characterized, we consider only extreme scenarios that illustrate the potential effects most clearly. Specifically, we consider only the fast replication regime of the previous section, which allows for a clear separation between nucleosome segregation and DNA filling with new nucleosomes (we do not need to consider the moving replication fork explicitly, but can use the deposited parental nucleosomes as an initial condition for the filling with *de novo* assembled nucleosomes). Furthermore, we assume the idealized case where a segregated nucleosome receives the same position on a daughter strand as it had on the parental DNA.

We focus on the question of how the filling kinetics are affected by the splitting process that distributes the parental nucleosomes between the two daughter strands, see 'Materials and Methods' section. Figure 6A depicts the two extreme cases of random distribution (bottom) and perfectly alternating distribution (top). Figure 6B and C show the corresponding filling kinetics, for the SoNG and the HaNG model, respectively. Figure 6B and C also show the filling curve for empty DNA as a reference (black lines). For the alternating initial distribution (red lines in Figure 6B and C) we observe that the density reaches its final value very quickly, avoiding jamming (for the HaNG model) and cramming (for the SoNG model). This is to be expected, given that all gaps have the correct size for one additional nucleosome. The gaps are quickly filled, re-establishing the equilibrium density with no need for rearrangements. For random allocation between strands (blue lines) there are gaps that have accommodated two or more nucleosomes on the parental DNA, which are then likely to become obstructed by 'bad parkers', thus leading to jamming. The effects of parental histone positions are more pronounced for the HaNG model where jamming is more severe than in the SoNG model. However, even for the SoNG model the final approach to the steady-state is considerably faster when nucleosome filling is guided by alternating nucleosome segregation.

DISCUSSION

Summary

Our model-based analysis has shown that the formation of dense nucleosome arrays is expedited by nucleosome softness, which can be attributed to nucleosome breathing and stepwise assembly, and by positional guidance obtained through the replication process. For the latter, we identified two different mechanisms, (i) positional guidance by a moving replication fork and (ii) positional guidance by segregated parental histones. Mechanism (i) provides optimal guidance, if the nucleosome assembly rate is matched to the speed of the replication fork. If, however, the replication machinery moves too fast to allow

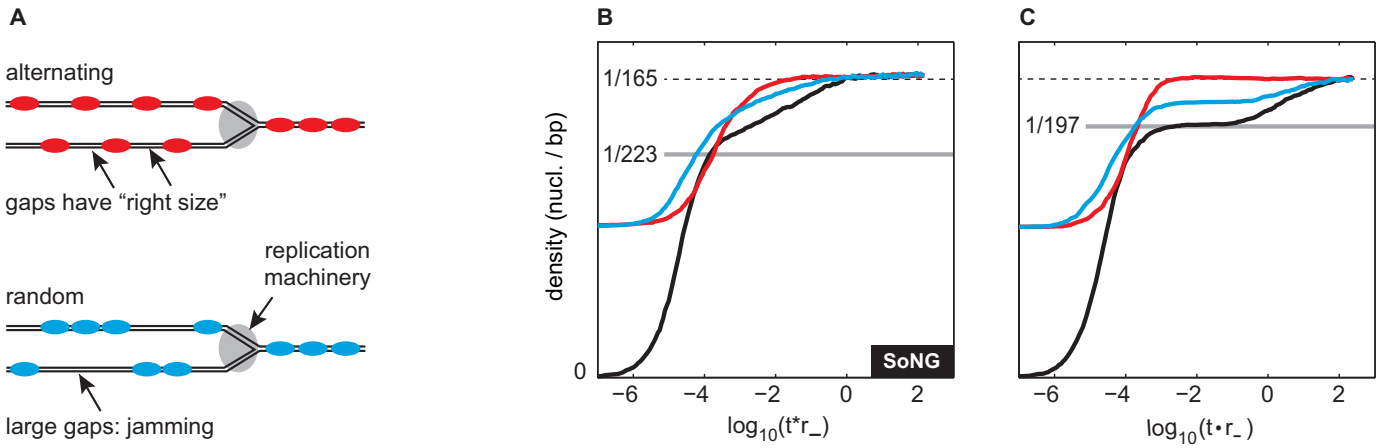

Figure 6. Effects of inherited parental nucleosome positions on filling dynamics. (**A**) An alternating distribution of parental nucleosomes onto the daughter strands ($\alpha = 1$) leads to gaps that each accommodate a single additional nucleosome (top panel), while a random distribution ($\alpha = 0.5$) leads to gaps of various sizes such that jamming will occur for *de novo* deposited nucleosomes (bottom panel). (**B**) Nucleosome filling dynamics of the SoNG model starting from an alternating inherited configuration (red), a random inherited configuration (blue) and from empty DNA as a reference (black). The dashed line marks the asymptotic density and the gray line the jamming density. (**C**) Same plot for the HaNG model.

dense packing in its wake, nucleosomes form at random positions, resulting in ‘jammed’ nucleosome configurations which must be resolved to further increase the DNA coverage. In this fast replication regime, mechanism (ii) can still prevent jamming. A caveat is that it is effective only if the segregated nucleosomes (approximately) retain their positions during DNA replication and neighboring nucleosomes on the parental DNA are typically segregated to different daughter strands. However, even if jammed nucleosome configurations do occur, we found that their effect on the nucleosome filling kinetics is much less dramatic for soft nucleosomes than when nucleosomes are approximated as hard-core particles.

We find it useful to illustrate replication-guided nucleosome packing by extending the ‘car parking’ analogy that is often used for one-dimensional adsorption-desorption models (11). Imagine a truck that slowly moves along the curb of a street, e.g. performing roadwork. Cars in search of parking spots can park right behind the truck as soon as the distance from the previously parked car is large enough. This results in densely spaced cars along the curb, analogous to the replication-guided filling described above. Now, assume that the truck moves by more than one car’s length before a driver looking for a parking spot arrives. Then, parking will no longer be ordered behind the truck. If however, the roadwork performed by the truck consists of painting parking spot guidelines on the road, dense packing is again established (assuming equal car lengths and drivers respecting guidelines). In the nucleosome context, such positioning guides emerge if the gaps between inherited nucleosomes correspond directly to the space vacated by a parental histone, such that each gap can be quickly filled by a single assembly event.

That nucleosomes with an effective soft-core interaction display much faster filling kinetics than hard-core nucleosomes is not a trivial effect. They are larger than their counterparts in the HaNG model and the interaction parameters are determined such that the same equilibrium density and compatible nucleosome patterns are obtained in both cases (24). Furthermore, the filling kinetics of the soft-core nucleosomes differs significantly from that of the hard-core nucleosomes: the latter quickly run into a stagnating nucleosome density, the ‘jamming plateau’, followed by a long period of collective rearrangements during which the nucleosome density creeps to the final steady-state density. In contrast, the density of soft-core nucleosomes does not plateau before reaching the final steady-state. Rather, the SoNG model displays a cramming stage, during which the nucleosome density steadily increases, followed by a rapid relaxation to the steady-state nucleosome pattern via nucleosome rearrangements that are guided by the nucleosome–nucleosome interaction. Taking nucleosome softness into account thus leads to profound effects that should not be ignored in kinetic studies of nucleosome array formation. For steady-state properties, the hard-core description (26) remains a useful abstraction that can even quantitatively describe the gene-averaged nucleosome pattern adjacent to nucleosome-free regions (51), albeit not in a unified way, across different species (24).

Assumptions and limitations

Taken together, our findings suggest that the biophysics of nucleosomes and DNA replication helps cells to avoid the kinetic problem of jamming, which would otherwise arise in the formation of dense nucleosome arrays (13). We note that the dramatic speedup of the filling kinetics of the soft-core model compared to the hard core model is a *generic* property of soft nucleosomes, i.e. it is robust to changes in the specific shape of the interaction potential. Clearly, our coarse-grained model has many simplifying assumptions, which could potentially affect this conclusion. For instance, our SoNG model is restricted to nearest-neighbor interactions between nucleosomes. While it is certainly possible to integrate longer-range interactions (mediated by higher-order chromatin structure) into these models (52), there is currently no experimental evidence that nearest-neighbor

interactions do not suffice to describe the statistical distribution of nucleosome positions. Another simplifying assumptions was to ignore the DNA sequence preferences of nucleosomes, which would make our on- and off-rates r_+ and r_- position-dependent. However, position-dependent rates can provide additional guidance and further reduce the tendency of nucleosomes to jam, i.e. the assumption is not critical.

One of the limitations of our study is the inability of our coarse-grained model to predict the absolute timescale of the nucleosome filling kinetics. A crucial unknown parameter is the *in vivo* rate of nucleosome assembly (the rate r_+ in our model). Using the *in vitro* estimate of (14), our SoNG model suggests that 90% DNA coverage can be reached on a timescale of several minutes, see Figure 3. However, this estimate has considerable uncertainty, due to both the extrapolation to zero applied force in (14) and the usage of an *in vitro* rate for an *in vivo* process. The strength of the coarse-grained modeling approach is that it can compare different mechanisms in terms of their relative speed of nucleosome array assembly. Our model comparison demonstrated that soft-core nucleosomes have a kinetic advantage over hard-core nucleosomes, with an almost two orders of magnitude shorter assembly time for nucleosome arrays with the spacing of *S. cerevisiae*. The SoNG assembly time is in fact comparable to the timescale estimated within a similar coarse-grained model for hard-core nucleosomes, but with remodeler-assisted nucleosome sliding (13) (passive nucleosome sliding without assistance by remodeling enzymes is too slow to significantly affect assembly times).

Our treatment of replication-guided nucleosome packing has introduced a minimal model for the simultaneous kinetics of DNA replication and assembly of nucleosome arrays.

Rather than modeling the detailed processes at the replication fork, we focused on the more general question of how the processive nature of replication influences filling kinetics. This establishes the basis upon which more elaborate orchestration of chromatin reassembly may operate. Slow progression of the replication fork compared to the nucleosome assembly rate helps to avoid nucleosome jamming, while the guiding effect of the fork is negligible at fast progression speeds. We showed that for very slow progression, the density in the wake of the fork even exceeds its equilibrium value temporarily. It is tempting to speculate whether a coupling mechanism between the assembly rate and the fork speed might allow cells to tune the replication-guided density to the steady-state value. This density would then be reached substantially faster than even the soft-core model predicts for the homogeneous case. An indication for such a feedback mechanism was indeed reported in mammalian cells: limiting the supply of new histones slows down the replication fork (53). However, in these experiments the nucleosome density on the nascent daughter strands was reduced in histone depleted conditions, indicating that the feedback mechanism might not fully compensate for the lower histone availability. To what extent this feedback might tune the ratio of speed and assembly toward the optimal regime is currently unclear.

We also investigated possible influences of histone segregation. Again, our model is certainly not meant as a full description of these processes in yeast cells. For instance, we have ignored differences between the replication of the leading and the lagging strand. Instead, our model serves to illustrate generic consequences of an interplay between the DNA replication machinery and nucleosome assembly. This interplay depends on the statistical properties of the nucleosome segregation process. Fast assembly of dense arrays is facilitated by an alternating deposition of parental nucleosomes to the daughter strands and a high correlation between parental nucleosome positions and those on the daughter strands. These aspects of DNA replication and nucleosome segregation are insufficiently characterized experimentally. However, it does seem clear already that the details are context-dependent. For instance, while nucleosomes are generally believed to be allocated in equal shares to the two daughter strands, nucleosomes in *Drosophila* germline stem cells are mainly segregated to one daughter strand, while *de novo* assembled nucleosomes are enriched on the other (38). It is also interesting to note that replication of the lagging strand was found to be tied to the assembly of nascent chromatin: Okazaki fragment lengths are multiples of the average nucleosome spacing in *S. cerevisiae* with fragments terminating preferentially at consensus dyad positions, and suppression of nucleosome assembly resulted in longer fragments (39).

Finally, our model does not explicitly account for remodeling enzymes, which are known to reposition, remove and restructure nucleosomes (18). As described in the model section, we incorporate the action of histone chaperones into our effective assembly rate r_+, and the ATP-assisted removal of nucleosomes in our effective eviction rate r_-. Note that the parameters of the potential which describes the reduced on-rate for overlapping adsorptions are determined from *in vivo* nucleosome positioning patterns that include the effects of remodelers. Our analysis has shown that reasonable effective rate constants r_+ and r_- are sufficient for rapid formation of dense nucleosome arrays, once nucleosome softness is taken into account. While our findings don't deny that other types of remodeling processes are also taking place, they suggest that active lateral repositioning of nucleosomes is not required to form dense nucleosome arrays in a timely manner. This conclusion is not in conflict with the observation that the reconstitution of nucleosome patterns across the 5' ends of yeast genes requires whole cell extract and ATP (54), given that eviction of nucleosomes is also ATP-assisted.

However, these and other experiments at reduced nucleosome density show that our model is not sufficient for a coherent quantitative description of gene-averaged nucleosome patterns for all experimental conditions. At a minimum, this will require either a mechanism that pushes nucleosome toward the 5′ ends of genes (54) or a mechanism that mediates a nucleosome–nucleosome attraction (24).

Experimental ramifications and outlook

Our theoretical analysis of replication-guided nucleosome packing stimulates several experimental questions. Given that the kinetically optimal scenario lies in the regime where the replication speed is tuned to the nucleosome assembly rate r_+ times the dyad-to-dyad spacing of the packed nucleosome array, it is of particular interest to test whether yeast

cells typically operate in this regime. The replication fork speed could even be controlled externally via hydroxyurea (55,35) to study different regimes of the wake filling mechanism *in vivo*. A useful experimental observable for comparison with theoretical models would be the nucleosome density profile as a function of the distance to the replication fork. This density profile should display a depletion zone behind the fork, whose width is a function of the ratio of the replication fork speed to the speed of nucleosome assembly.

The process of nucleosome segregation has been of great interest in the context of epigenetic inheritance of histone modifications. Our theoretical analysis has shown that the statistical properties of this process can also have strong effects during the process of reforming dense nucleosome arrays after DNA replication. An experimental analysis of these statistical properties could simultaneously shed new light on both questions and would be highly desirable. We hope that a dynamical analysis of nucleosome arrays will significantly advance our quantitative understanding of the processes that shape the arrays.

SUPPLEMENTARY DATA

Supplementary Data is available at NAR Online.

FUNDING

Bavarian Research Network for Molecular Biosystems (BioSysNet); Nanosystems Initiative Munich (NIM); Funding for open access charge: Ulrich Gerland.
Conflict of interest statement. None declared.

REFERENCES

1. Venkatesh,S., Workman,J.L. and Smolle,M. (2013) UpSETing chromatin during non-coding RNA production. *Epigenetics Chromatin*, **6**, 16.
2. Svaren,J. and Hoerz,W. (1997) Transcription factors vs nucleosomes: regulation of the PHO5 promoter in yeast. *Trends Biochem. Sci.*, **22**, 93–97.
3. Bai,L. and Morozov,A.V. (2010) Gene regulation by nucleosome positioning. *Trends Genet.*, **26**, 476–483.
4. Bell,O., Tiwari,V.K., Thomä,N.H. and Schübeler,D. (2011) Determinants and dynamics of genome accessibility. *Nat. Rev. Genet.*, **12**, 554–564.
5. Rando,O. and Winston,F. (2012) Chromatin and transcription in yeast. *Genetics*, **190**, 351–387.
6. Jiang,C. and Pugh,B.F. (2009) A compiled and systematic reference map of nucleosome positions across the Saccharomyces cerevisiae genome. *Genome Biol.*, **10**, R109.
7. Yuan,G., Liu,Y., Dion,M.F., Slack,M.D., Wu,L.F., Altschuler,S.J. and Rando,O.J. (2005) Genome-scale identification of nucleosome positions in S. cerevisiae. *Science*, **309**, 626–630.
8. Jiang,C. and Pugh,B.F. (2009)(2009) Nucleosome positioning and gene regulation: advances through genomics. *Nat. Rev. Genet.*, **10**, 161–172.
9. Evans,J.W. (1993) Random and cooperative sequential adsorption. *Rev. Mod. Phys.*, **65**, 1281–1329.
10. Jin,X., Tarjus,G. and Talbot,J. (1994) An adsorption-desorption process on a line: kinetics of the approach to closest packing. *J. Phys. A*, **27**, L195–L200.
11. Krapivsky,P.L. and Ben-Naim,E. (1994) Collective properties of adsorption–desorption processes. *J. Chem. Phys.*, **100**, 6778–6782.
12. Rényi,A. (1963) On a one-dimensional problem concerning random space filling. *Sel. Trans. Math. Stat. Prob.*, **4**, 203–218.
13. Padinhateeri,R. and Marko,J.F. (2011) Nucleosome positioning in a model of active chromatin remodeling enzymes. *Proc. Natl. Acad. Sci. U.S.A.*, **108**, 7799–7803.
14. Padinhateeri,R., Yan,J. and Marko,J.F. (2007) Nucleosome hopping and sliding kinetics determinedfrom dynamics of single chromatin fibers in Xenopus egg extracts. *Proc. Natl. Acad. Sci. U.S.A.*, **104**, 13649–13654.
15. Polach,K.J. and Widom,J. (1995) Mechanism of protein access to specific DNA sequences in chromatin: a dynamic equilibrium model for gene regulation. *J. Mol. Biol.*, **254**, 130–149.
16. Li,G. and Widom,J. (2004) Nucleosomes facilitate their own invasion. *Nat. Struct. Mol. Biol.*, **11**, 763–769.
17. Buning,R. and van Noort,J. (2010) Single-pair FRET experiments on nucleosome conformational dynamics. *Biochimie*, **92**, 1729–1740.
18. Clapier,C.R. and Cairns,B.R. (2009) The biology of chromatin remodeling complexes. *Annu. Rev. Biochem.*, **78**, 273–304.
19. Flaus,A. and Owen-Hughes,T. (2004) Mechanisms for ATP-dependent chromatin remodelling: farewell to the tuna-can octamer? *Curr. Opin. Genet. Dev.*, **14**, 165–173.
20. Fan,H., He,X., Kingston,R.E. and Narlikar,G.J. (2003) Distinct strategies to make nucleosomal DNA accessible. *Mol. Cell*, **11**, 1311–1322.
21. Kassabov,S.R., Zhang,B., Persinger,J. and Bartholomew,B. (2003) SWI/SNF unwraps, slides, and rewraps the nucleosome. *Mol. Cell*, **11**, 391–403.
22. Akey,C.W. and Luger,K. (2003) Histone chaperones and nucleosome assembly. *Curr. Opin. Struct. Biol.*, **13**, 6–14.
23. Engeholm,M., de Jager,M., Flaus,A., Brenk,R., van Noort,J. and Owen-Hughes,T. (2009) Nucleosomes can invade DNA territories occupied by their neighbors. *Nat. Struct. Mol. Biol.*, **16**, 151–158.
24. Moebius,W., Osberg,B., Tsankov,A.M., Rando,O.J. and Gerland,U. (2013) Toward a unified physical model of nucleosome patterns flanking transcription start sites. *Proc. Natl. Acad. Sci. U.S.A.*, **110**, 5719–5724.
25. Chereji,R.V. and Morozov,A.V. (2014) Ubiquitous nucleosome crowding in the yeast genome. *Proc. Natl. Acad. Sci. U.S.A.*, **111**, 5236–5241.
26. Kornberg,R.D. and Stryer,L. (1988) Statistical distribution of nucleosomes: nonrandom locations by a stochastic mechanism. *Nucleic Acids Res.*, **16**, 6677–6690.
27. Parmar,J.J., Marko,J.F. and Padinhateeri,R. (2014) Nucleosome positioning and kinetics near transcription-start-site barriers are controlled by interplay between active remodeling and DNA sequence. *Nucleic Acids Res.*, **42**, 128–136.
28. Raghuraman,M.K., Winzeler,E.A., Collingwood,D., Hunt,S., Wodicka,L., Conway,A., Lockhart,D.J., Davis,R.W., Brewer,B.J. and Fangman,W.L. (2001) Replication dynamics of the yeast genome. *Science*, **294**, 115–121.
29. Gruss,C., Wu,J., Koller,T. and Sogo,J.M. (1993) Disruption of the nucleosomes at the replication fork. *EMBO J.*, **12**, 4533–4545.
30. Groth,A., Rocha,W., Verreault,A. and Almouzni,G. (2007) Chromatin challenges during DNA replication and repair. *Cell*, **128**, 721–733.
31. MacAlpine,D.M. and Almouzni,G. (2013) Chromatin and DNA replication. *Cold Spring Harbor Perspect. Biol.*, **5**, a010207.
32. Whitehouse,I. and Smith,D.J. (2013) Chromatin dynamics at the replication fork: there's more to life than histones. *Curr. Opin. Genet. Dev.*, **23**, 140–146.
33. Sogo,J.M., Stahl,H., Koller,T. and Knippers,R. (1986) Structure of replicating simian virus 40 minichromosomes. The replication fork, core histone segregation and terminal structures. *J. Mol. Biol.*, **189**, 189–204.
34. Radman-Livaja,M., Verzijlbergen,K.F., Weiner,A., van Welsem,T., Friedman,N., Rando,O.J. and van Leeuwen,F. (2011) Patterns and mechanisms of ancestral histone protein inheritance in budding yeast. *PLoS Biol.*, **9**, e1001075.
35. Rodriguez,J. and Tsukiyama,T. (2013) ATR-like kinase Mec1 facilitates both chromatin accessibility at DNA replication forks and replication fork progression during replication stress. *Genes Dev.*, **27**, 74–86.
36. Pospelov,V., Russev,G., Vassilev,L. and Tsanev,R. (1982) Nucleosome segregation in chromatin replicated in the presence of cyclohexamidine. *J. Mol. Biol.*, **156**, 79–91.
37. Annunziato,A.T. (2005) Split decision: what happens to nucleosomes during DNA replication? *J. Biol. Chem.*, **280**, 12065–12068.

38. Tran,V., Lim,C., Xie,J. and Chen,X. (2012) Asymmetric division of Drosophila male germline stem cell shows asymmetric histone distribution. *Science*, **338**, 679–682.
39. Smith,D.J. and Whitehouse,I. (2012) Intrinsic coupling of lagging-strand synthesis to chromatin assembly. *Nature*, **483**, 434–438.
40. Anderson,J.D. and Widom,J. (2000) Sequence and position-dependence of the equilibrium accessibility of nucleosomal DNA target sites. *J. Mol. Biol.*, **296**, 979–987.
41. Mazurkiewicz,J., Kepert,J.F. and Rippe,K. (2006) On the mechanism of nucleosome assembly by histone chaperone NAP1. *J. Biol. Chem.*, **281**, 16462–16472.
42. Ransom,M., Dennehey,B.K. and Tyler,J.K. (2010) Chaperoning histones during DNA replication and repair. *Cell*, **140**, 183–195.
43. Annunziato,A.T. (2012) Assembling chromatin: the long and winding road. *Biochim. Biophys. Acta*, **1819**, 196–210.
44. Liu,W.H. and Churchill,M.E.A. (2012) Histone transfer among chaperones. *Biochem. Soc. Trans.*, **40**, 357–363.
45. Korber,P., Luckenbach,T., Blaschke,D. and Horz,W. (2004) Evidence for histone eviction in trans upon induction of the yeast PHO5 promoter. *Mol. Cell. Biol.*, **24**, 10965.
46. Boeger,H., Griesenbeck,J., Strattan,J.S. and Kornberg,R.D. (2004) Removal of promoter nucleosomes by disassembly rather than sliding in vivo. *Mol. Cell.*, **14**, 667–673.
47. Korber,P. (2012) Active nucleosome positioning beyond intrinsic biophysics is revealed by in vitro reconstitution. *Biochem. Soc. Trans.*, **40**, 377–382.
48. Schiessel,H. (2003) The physics of chromatin. *J. Phys.: Condens. Matter*, **15**, R699–R774.
49. Gillespie,D.T. (1977) Exact stochastic simulation of coupled chemical reactions. *J. Phys. Chem.*, **81**, 2340–2361.
50. Yan,J., Maresca,T.J., Skoko,D., Adams,C.D., Xiao,B., Christensen,M.O., Heald,R. and Marko,J.F. (2007) Micromanipulation studies of chromatin fibers in *Xenopus* egg extracts reveal ATP-dependent chromatin assembly dynamics. *Mol. Biol. Cel*, **18**, 464–474.
51. Möbius,W. and Gerland,U. (2010) Quantitative test of the barrier nucleosome model for statistical positioning of nucleosomes up- and downstream of transcription start sites. *PLoS Comput. Biol.*, **6**, e1000891.
52. Chereji,R.V. and Morozov,A.V. (2011) Statistical mechanics of nucleosomes constrained by higher-order chromatin structure. *J. Stat. Phys.*, **144**, 379–404.
53. Mejlvang,J., Feng,Y., Alabert,C., Neelsen,K.J., Jasencakova,Z., Zhao,X., Lees,M., Sandelin,A., Pasero,P., Lopes,M. *et al.* (2014) New histone supply regulates replication fork speed and PCNA unloading. *J. Cell Biol.*, **204**, 29–43.
54. Zhang,Z., Wippo,C.J., Wal,M., Ward,E., Korber,P. and Pugh,B.F. (2011) A packing mechanism for nucleosome organization reconstituted across a eukaryotic genome. *Science*, **332**, 977–980.
55. Poli,J., Tsaponina,O., Crabbé,L., Keszthelyi,A., Pantesco,V., Chabes,A., Lengronne,A. and Pasero,P. (2012) dNTP pools determine fork progression and origin usage under replication stress. *EMBO J.*, **31**, 883–894.